ONLINE SUPPLEMENT

Author Contributions

Joshua Harrill—experimental designs; performed the experiments; prepared all drafts of the manuscript and with LM Reid the final version of the manuscript.

Bethany Parks—helped with the cultures and with the high content image analyses.

Eliane Wauthier—helped with the cultures and with development of the culture conditions for the rat hepatic stem cells versus hepatoblasts

Craig Rowlands—helped with the experimental design in terms of choices of AHR agonists and analyses of the AHR.

Rusty Thomas—experimental designs especially for the toxicological studies; helped with editing of the manuscript; funding of the studies

Lola Reid—experimental designs; determined the conditions for cultures of stem cells versus hepatoblasts and helped with the analyses of stem/progenitor cell properties; helped with all drafts of the manuscript especially the final rounds of editing to prepare the manuscript for submission for publication and with all drafts for the revision; funding of the studies

Abbreviations

AFP**,** alpha-fetoprotein; **AHR**, aryl hydrocarbon receptor; **ARNT**, aryl hydrocarbon receptor nuclear translocator; **AHRR**, aryl hydrocarbon receptor repressor; **bHLH/PAS**, basic-helix-loop-helix/Per-ARNT-Sim transcription factor;; **CD133,** prominin 1**; CS-PG,** chondroitin sulfate proteoglycan; **CXCR4**, CXC-chemokine receptor 4; **CYP450**, Cytochrome p450s; **DIM,** 3-3'-diindolylmethane; **DREs**, dioxin-response elements; **DS-PG**, dermatan sulfate proteoglycan; **EGF**, epidermal growth factor; **EpCAM**, epithelial cell adhesion molecule; **FBS**, fetal bovine

serum; **FICZ,** 6-formylindolo-[3,2-b]carbazole; **GAGs**, glycosaminoglycans; **HA,** hyaluronan; **HB,** human hepatoblast; **HDM**, serum-free, hormonally defined medium; **HEP**, hepatocyte; **HGF**, hepatocyte growth factor; **HpSC,** hepatic stem cells; HSP90/AIP/p23, heat shock protein 90/AJP/23 multiprotein chaperone complex; **HS-PG**, heparan sulfate proteoglycan; **ICAM1,** intercellular adhesion molecule-1; **KM**, Kubota's Medium, a serum-free medium designed for endodermal stem/progenitors; **LIF**, leukemia inhibitory factor; **LGR5**, leucine-rich repeat-containing G protein coupled receptor 5 ; **NCAM**, neural cell adhesion molecule; **PBG**, peribiliary gland; **SALL4,** Sal-like protein 4; **SMA,** alpha-smooth muscle actin; **SOX,** Sry-related HMG box; **TCDD**, 2,3,7,8-tetrachlorodibenzodioxin; **VEGF,** vascular endothelial cell growth factor.

Phenotypic Properties (Biomarkers) for Lineage Stages of Parenchymal Cells. Below is given a summary regarding lineage-dependent properties of parenchymal cells in mammalian biliary trees and livers, with a focus on early lineage stages in rat livers. The information on the biliary tree stem cell populations is entirely from human studies, since these populations in rats and mice have yet to be characterized. The statements paraphrase those from refereed articles and reviews on biliary tree stem cells, hepatic stem cells and hepatoblasts and on their mesenchymal partners. These statements are presented in tabular form in **Table S3.** An especially succinct summary is given regarding the adult descendants of the stem progenitors: the plates of hepatocytes, cholangiocyes and mesenchymal cells found within the acinus from the periportal to pericentral zones; for more details, see the articles and reviews referenced (1-13)

All tissues are organized as partnerships between epithelial and mesenchymal cells and, in parallel, in maturational lineages of these partners going from stem cells, transitioning through intermediates, to lineage stages of adult cells, and finally to apoptotic cells. The stem cell niches contain stem cells, multipotent and with self-replicative ability, and committed progenitors, unipotent cells that are highly proliferative but without an ability for self-replication. The stem cells give rise to daughter cells, maturing step-wise with lineage-dependent cell size, morphology, ploidy, proliferative potential, antigenic profile and tissue-specific gene expression. The lineage kinetics and tissue turnover rates are tissue-specific and correlate inversely with the extent of polyploidy. Fetal and neonatal liver tissues are entirely diploid. The transition to adult ploidy profiles in liver occurs within 3 weeks in mice; within 4 weeks in rats; and by late teenage years in humans; and the extent of polyploidy increases with age. The profile is distinct in different species. For example, adult human livers are mostly diploid (>80%) and with the remainder being tetraploid (10-20%). By contrast, adult rat livers at 4 weeks of age are ~10% diploid, ~80% tetraploid, and ~10% octaploid. In all mammalian

species the diploid cells within the liver acinus are found periportally transitioning to polyploid cells near to the central vein (and in rodent species, polyploid cells are also mid-acinar). Ploidy profiles of the extrahepatic biliary tree cells have yet to be studied.

The maturational lineages for liver (and for pancreas) begin in the biliary tree near the duodenum in the hepato-pancreatic common duct, the site of the highest numbers of very primitive stem cells. The path of the maturational lineages is along the biliary tree and parallels that found in developing liver and pancreas. The stem cell niches in most of the biliary tree are peribiliary glands (PBGs) found within the walls of the bile ducts (intramural PBGs) or tethered to the duct walls (extramural) (10); the exception is in the gallbladder that has no PBGs and in which the niches are organized more like those in the intestine with crypts that connect to villi(14). These PBGs connect into the intra-hepatic stem cell niches, the canals of Hering(15), located periportally in the liver acini, and into the intra-pancreatic niches, pancreatic duct glands (PDGs), comprised entirely (or almost entirely) of committed progenitors(16).

There are multiple subpopulations of biliary tree stem cells (BTSCs) with the most primitive ones being in PBGs near the fibromuscular layers within bile ducts; transitioning to intermediates and then to mature cells with location of the PBGs nearing to the lumen of the bile ducts(16, 17). The earliest stages of these lineages (those near the fibromuscular layers) consist of cells that strongly express endodermal transcription factors (SOX9, SOX17, PDX1), pluripotency genes (e.g. OCT4, SOX2, KLF4, NANOG), various other stem cell markers (e.g. CD44, CD133, hedgehog proteins, aldehyde dehydrogenase-ALDH, SALL4), but with <u>no</u> expression of LGR5 or EpCAM or of mature markers (either hepatic or pancreatic) (10, 14-17). Intermediate stages of biliary tree stem cell populations express some but not all of the endodermal transcription factors (e.g. SOX9 and either SOX17 or PDX1 but not both); lower levels of the pluripotency genes and stem cell markers; CD44, LGR5 and EpCAM, but still not

mature cell markers. With increasing proximity to the lumens of the bile ducts, the stem cell traits fade, and mature markers appear and increase in level of expression. If the microenvironment is near the liver, the mature markers that emerge are hepatic; if near the pancreas, the mature markers are pancreatic; and in-between, they are bile duct. The mesenchymal cell partners of the now at least 3 major stages of biliary tree stem cell subpopulations have yet to be defined.

The intrahepatic stem cell niches comprise the ductal plates in fetal and neonatal developmental stages, transitioning to canals of Hering in pediatric and adult stages(18). They contain hepatic stem cells (7-9 μm), partnered tightly with angioblasts (positive expression for CD117, CD133, VEGF-receptor, and Van Willebrand Factor). The stem cells and their partners, angioblasts, are connected to hepatoblasts, that are partnered with endothelial cell precursors (positive expression for CD133, VEGF-receptor, Van Willebrand Factor, and CD31) and to stellate cell precursors (positive expression for CD146, ICAM-1, desmin, alpha-smooth muscle actin, beta-3-integrin and low levels of vitamin A but no glial fibrillary acidic protein-GFAP) (7, 18-21). The mesenchymal cells produce critical paracrine signals(21).

The hepatic stem cells in humans express SOX9, SOX17; low levels of pluripotency genes (OCT4, KLF4, NANOG); other stem cell markers (hedgehog proteins, CD44, ALDH, CD133); strong levels throughout the cell of EpCAM and NCAM but no alpha-fetoprotein (AFP) and minimal (if any) albumin (6, 7, 19, 21). Interestingly, telomerase protein is found entirely within the nucleus, and telomerase activity occurs at basal levels (22) .

These hepatic stem cells are precursors to hepatoblasts (10-12 μm) that are devoid of SOX17 (faint, if any, SOX9), devoid of the pluripotency genes and of NCAM, and yet expression of other stem cell markers (CD44, CD133, hedgehog proteins). Telomerase is found within the nucleus as well as cytoplasmically, and its activity levels are at least 5-fold higher than those in the hepatic stem cells (22). Positive strong expression is found in

hepatoblasts for AFP, LGR5, ICAM-1, and P450A7 but with EpCAM now confined to the plasma membrane (7, 18, 19). In fetal and neonatal livers, the majority of the parenchymal cells are hepatoblasts; in adult livers, the hepatoblasts are very few and found as individual cells between stem cells and periportal hepatocytes or cholangiocytes (18, 23, 24). Known stages for stem/progenitors are given below in a figure modified from one published previously (10, 11). (See also **Figure S3**).

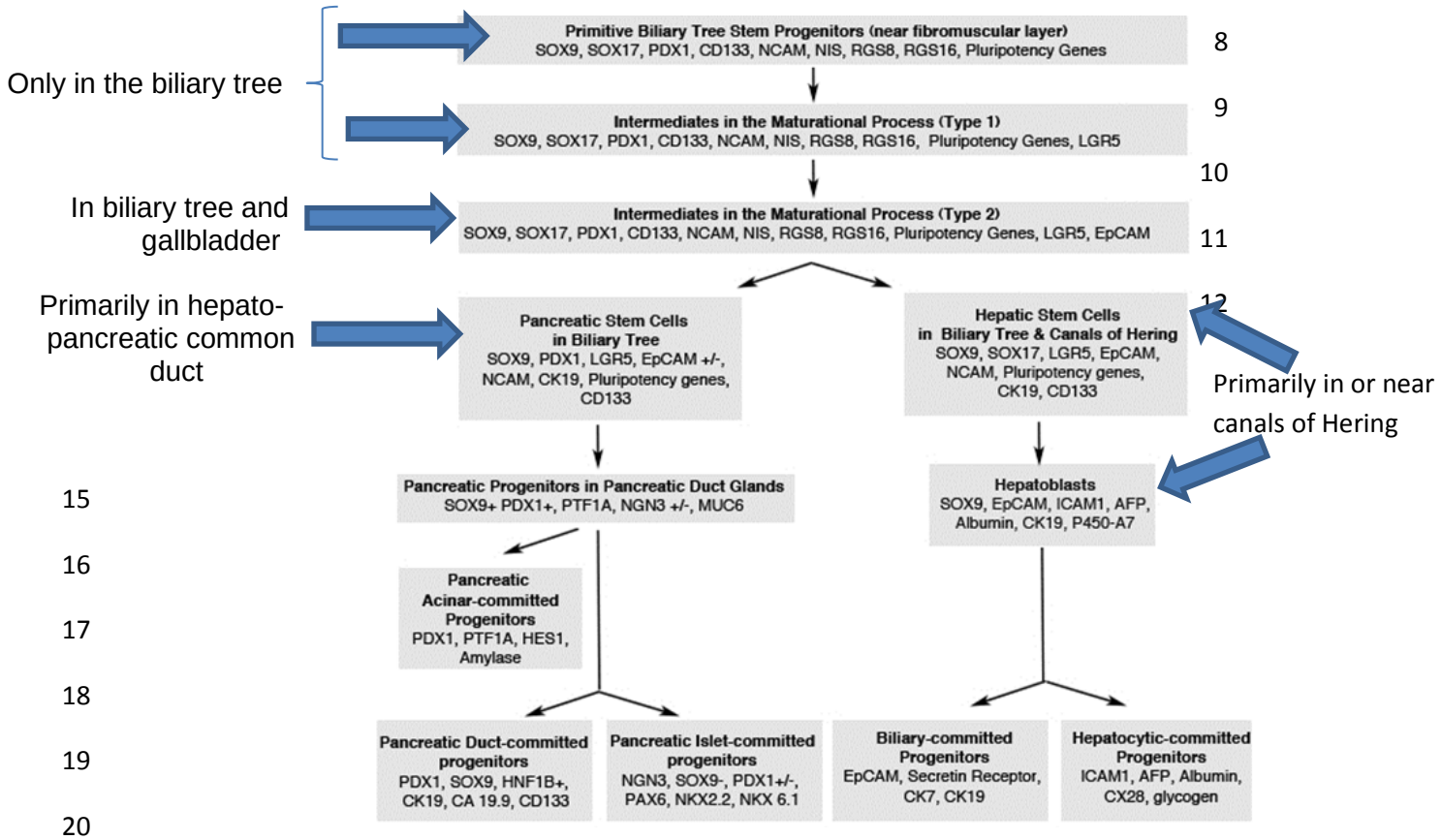

Pluripotency genes include: SOX2, OCT4, KLF4, NANOG, TROP-2, BMi-1, and SALL4. Cells at all stages express cytokeratins 8 and 18. NIS=sodium iodide symporter.

<u>Intrahepatic lineage stages</u>- The zonal distribution of the liver's known heterogeneity of functions has been described extensively in the past and is summarized in a number of articles and reviews (1, 2, 4, 6, 25-29) . Here is a brief summary of major changes in the phenotypic traits and found in a zonal distribution pattern correlating with the maturational

lineages:

Periportal parenchymal cells (zone 1) in rats are comprised of “small hepatocytes” and intrahepatic biliary epithelia, or “large cholangiocytes”; these are entirely diploid and with diameters that are ~18 μm for hepatocytes and ~14 μm for cholangiocytes. The hepatocytes form plates or cords of cells closely associated with sinusoidal endothelia that in zone 1 are continuous and linked to each other. The periportal hepatocytes peak in factors and enzymes associated with gluconeogenesis, amino acid and ammonia metabolism, urea synthesis, and glutathione peroxidase. Although many of the genes expressed are regulated fully transcriptionally and posttranscriptionally, there are some (e.g. transferrin) in which the mRNA is expressed but not translated and others (e.g. albumin) in which only some of the known transcriptional regulator mechanisms influencing albumin are operative.

Midacinar parenchymal cells (zone 2). In rats, midacinar hepatocytes are tetraploid, are larger (>22-25 μm) and contain genes that all regulate fully both transcriptionally and posttranscriptionally. The mRNA for transferrin is expressed at most (possibly all?) early lineage stages, but there is no transferrin protein produced until the midacinar lineage stages, since critical factors needed for translation appear at these stages. There are parallel examples of lineage dependence of particular transcription factors or factors needed for mRNA half-life and that become fully operative in the mid-acinar zone.

Pericentral parenchymal cells (zone 3) In rats, the pericentral zone contains hepatocytes that are a mix of tetraploid and octaploid cells, and comprise the largest

parenchymal cells in the liver (e.g. >30 μM in rats). These transition to cells undergoing apoptosis and that are easily recognizable with TUNEL assays and others indicating DNA fragmentation (30, 31). The gene expression profile includes late P450s, glutathione transferases, UDP-glucuronyl-transferases, glutamine synthetase and heparin proteoglycans, and the zone 3 region is replete with Kupfer cells that are known to participate in removal of apoptotic cells. The endothelia of zone 3 are no longer continuous but rather are fenestrated such that the parenchymal cells are in direct contact via their extracellular matrix with blood. (32, 33).

Methods

Materials. Recombinant rat leukemia inhibitory factor (rat ESGRO®) and Bisbenzimide H 33258 fluorochrome (Hoeschst stain) was purchased from EMD-Millipore (Billerica, MA). Optiprep™, Hyaluronic acid sodium salt from *Streptococcus equi*, Collagenase from *Clostridium histolyticum*, DNase from bovine pancreas and all additive components of Kubota's media (see below) except for zinc sulfate heptahydrate and L-glutamine were purchased from Sigma-Aldrich (St. Loius, MO). SpecPure® Zinc sulfate heptahydrate was purchased from Alfa Aesar (Ward Hill, MA). GIBCO® DMEM, RPMI 1640, L-glutamine and antibiotic / antimycotic cocktail and AlexaFluor conjugated secondary antibodies were purchased from Life Technologies (Grand Island, NY). Normal donkey serum was purchased from Jackson ImmunoResearch Laboratories (West Grove, PA). Suppliers for immunocytochemistry primary antibodies are listed in **Supplementary Table 1**. RLT Buffer and RNEasy Mini Kits were purchased from Qiagen (Germantown, MD). Applied Biosystems™ TaqMan® Gene Expression Assays and TaqMan® RNA-to-Ct™ 1-Step Kits were purchased from Life Technologies.

2,3,7,8-tetrachlorodibenzo-p-dioxin (TCDD) was purchased from AccuStandard (New Haven, CT). 6-formylindolo[3,2-b]carbazole (FICZ) was purchased from Enzo Life Sciences

(Exeter, UK). 3,3'-diindolylmethane (DIM) was purchased from Sigma-Aldrich. Chemicals structures for these agonists are presented in **Figure S1.**

Kubota's medium (KM) is a serum-free, wholly defined medium designed for endodermal stem/progenitors and was first developed in the isolation of rHBs (8, 34). It subsequently was found effective for expansion of human hepatic stem cells (hHpSCs) and hepatoblasts (hHBs) as well as for multiple subpopulations of human biliary tree stem cells (hBTSCs) (7, 14-19, 35, 36). It is comprised of basal medium, low calcium, no copper, insulin, transferrin, and a mixture of lipids, and is devoid of cytokines or growth factors. KM contains RPMI 1640 media supplemented with the following: bovine serum *albumin* (1 mg/mL), L-glutamine (2 mM), nicotinamide (0.54 mg/mL), insulin (5 ug/mL), transferrin (10 ug/mL), hydrocortisone (100 nM), selenium (30 nM), zinc sulfate (1 nM), β-mercaptoethanol (50 uM), palmitic acid (31 mM), palmitoleic acid (2.8 mM), stearic acid (11.6 mM), oleic acid (13.4 mM), linoleic acid (35.6 mM) and linoleic acid (5.6 mM) plus an antibiotic / antimycotic cocktail. In culture, the growth of endodermal stem/progenitors from all species tested has been successful with KM. The clonogenic expansion of the HpSCs is dependent on partially identified and unidentified paracrine signals from angioblast feeders (but not stellate cell feeders) and that form close spatial associations with the expanding hepatic stem cell colonies (7, 21). The hepatoblasts have feeders of endothelial and stellate cell precursors that provide distinct matrix and soluble paracrine signals(20, 21, 34, 37, 38).

Rat Hepatic Stem / Progenitor Cell Cultures. Postnatal day 0-2 female Sprague Dawley rat livers were purchased from Charles River, Inc. (Wilmington, MA). Livers were stored in chilled Dulbecco's modified eagles medium (DMEM) supplemented with an antibiotic / antimycotic cocktail containing amphotericin B, streptomycin and penicillin (Life Technologies Inc., Grand

Island, NY) and processed within 2 h after harvest. Livers (n = 6-12 / preparation) were minced, and tissue was suspended in DMEM supplemented with 0.6 mg / mL Collagenase (~300 U/mL) and 0.3 mg / mL DNase. Tissue was then digested for 40 minutes at 34°C with intermittent mixing every 10 minutes. Cells were allowed to settle for the final 5 minutes of digestion. The supernatant was then transferred to a fresh tube, pelleted by centrifugation at 250x*g* for 5 minutes, resuspended in fresh DMEM and stored at room temperature. Cells remaining in the original digestion tube were resuspended in fresh Collagenase / DNase media and digested for an additional 40 minutes at 34°C with intermittent mixing. Cells from the second digestion were pelleted by centrifugation at 250*x*g for 5 minutes, resuspended in fresh DMEM and combined with cells pelleted from the supernatant of the initial digestion. Cells were then filtered through a 70 µm nylon cell strainer and pelleted by centrifugation at 250*x*g for 5 minutes. Cells were then resuspended in a chilled 34% Optiprep solution prepared using Kubota's media (KM) + 0.3 mg/mL DNase. Cells were then centrifuged at 1400*x*g for 15 minutes at 4°C. Cells present at the Optiprep interface were transferred to a fresh tube with a plastic Pasteur pipette, resuspended in KM and filtered through 40 µm nylon cell strainer. A small aliquot of cells was diluted 1:10 in KM + 0.04% Trypan blue and counted in a hemocytometer to determine cell concentrations in suspension. Trypan blue positive cells and red blood cells were excluded during cell counting.

On the day prior to culture, six-well culture plates were filled with a solution of 0.144 mg/mL hyaluronic acid sodium salt (2 mL / well) in sterile de-ionized water and allowed to air-dry overnight in a laminar flow hood, resulting in a plating surface coated with 30 µg/cm^2 hyaluronan. Plates were re-hydrated with DMEM prior to seeding of cells. Cells were seeded at a density of 3x10^6 cells / well in KM containing recombinant rat leukemia inhibitory factor (LIF) at the concentrations specified in the individual experiments. Cells were allowed a 2 day attachment period. At 2 days *in vitro* (DIV) a media change with fresh KM + LIF was performed

to remove cells not bound to the plating surface. Additional media changes with KM + LIF were performed every 3 days.

In experiments examining the effects of aryl hydrocarbon receptor (AHR) agonists (TCDD, FICZ and DIM), dosing solutions of each chemical to be tested were prepared in 100% DMSO at a 1000x concentration. Chemicals were administered by addition of 1 µL of dosing solution per 1 mL of media to be added to the well at time of media change. The DMSO concentration in treated and vehicle control wells was 0.1%. In experiments examining AHR activation via Cyp1a1 induction, chemical was administered at 12 days in culture in Kubota's media + 1 ng/mL LIF. Cultures were sampled at 4, 24, 48 and 96 h after dosing. In experiments examining the effects of AHR agonists on hepatic stem/progenitor cell growth, chemical was administered at 2 days in culture and re-administered at each media change (5,8 and 11 days). Cultures were sampled at 12 days.

Immunocytochemistry. Media was aspirated and cultures were fixed in chilled methanol-acetone (1:1) for 10 minutes at 4°C. Cultures were then rinsed 3X with PBS and blocked for 1 h at 25°C with 5% normal donkey serum. Cultures were then rinsed 3X with PBS and incubated for 2 h at 25°C with primary antibodies diluted in PBS as described in Table S1. Cultures were rinsed with three times with PBS and incubated for 1 h at 25° C with a 1:1000 dilution of AlexaFluor conjugated donkey anti-IgG secondary antibodies diluted in PBS as listed in **Table S1.** Secondary antibody labeling solutions also contained 3 µg / mL Hoechst 33528 for visualization of cell nuclei. Cultures were then rinsed 4X with PBS with the final rinse serving as a storage buffer. Plates were sealed with an adhesive film and stored at 4°C, protected from light, prior to imaging. Antibodies are listed in **Table S1**. For high content image analysis studies, cultures were labeled for albumin and E-cadherin with a Hoechst 33528 nucleus stain.

High Content Image Analysis. High-content image analysis was performed on rat hepatic stem/progenitor cultures prepared in six-well plates and immunolabeled with E-cadherin-AlexaFluor 488, albumin-AlexaFluor 546, desmin-AlexaFluor 647 and Hoecsht 33528. Images were acquired using a BD Pathway 435 Bioimager (BD Biosciences, San Jose, CA) with an Olympus CPlanFl 10X (0.3 NA) objective. Within each well, 32 non-overlapping, unique fields-of-view were imaged across the plating surface. Matching 4 x 4 image montages were captured in each unique field-of-view, corresponding to the described fluorescent labels. Tagged image format (TIF) files were then analyzed using optimized Cellomics Morphology Explorer Bioapplication protocols (Thermo Scientific, Waltham, MA). Two protocols were designed for the purposes of the present study as described in **Figure S3** and **Figure S4**.

The first protocol utilized images of E-cadherin, albumin and Hoechst 33528 labeled cultures to quantify and characterize the growth of hepatic stem/progenitor cells (**Figure S3**). Hepatic stem/progenitor colonies were identified based upon E-cadherin labeling. Geometric and signal intensity-based measurements for each colony identified were reported for each individual colony. Measurements reported in the present study include colony area (μm^2, based on E-cadherin labeling), the number of stem/progenitor cells in a colony (based on the number of nuclei counted within each colony) and the fluorescent surface area density (FSAD) for both E-cadherin and albumin labeling. FSAD is a textural measurement which summarizes the intensity and variation in fluorescent pixel intensity across the area of an identified object. The second protocol utilized images of desmin and Hoechst 33528 labeled cells to quantify the growth of stellate precursor cells (**Figure S4**). Measurements of interest were areas of desmin-positive cells (μm^2) and the total number of *desmin*-positive cells per well.

Quantitative reverse transcription polymerase chain reaction (qRT-PCR) analysis. At the time of sampling, media was aspirated from cultures and were lysed with 600 µL of Qiagen RLT Buffer. Lysates were transferred to a RNase / DNase-free polypropylene tube and stored at -80°C prior to total RNA extraction. Total RNA was purified using a Qiagen RNEasy® Mini Kit according to manufacturer's protocol. Total RNA was eluted with DNase-free water and total RNA concentrations were quantified using a NanoDrop 2000 spectrophotometer (Thermo Scientific). Total RNA concentrations were then adjusted to an equivalent value with DNase-free water prior to qRT-PCR analysis. qRT-PCR was performed on an Applied Biosystems™ 7900HT Sequence Detection System (Life Technologies) using TaqMan® Gene Expression Assays and TaqMan® RNA-to-Ct™ 1-Step Kits according to manufacturer's recommended protocols. Reactions were performed in a 384-well plate at a 20 µL reaction volume. Thermal cycling conditions were as follows: 48°C for 15 min followed by 95°C for 10 min and 40 cycles of 95°C for 15 sec and 60°C for 1 min.

Details of gene expression assays used in this study are listed in **Table S2.** Data were analyzed using the 2(-Delta Delta C(T) method(39). *Rps18* was used as the internal reference gene in 2(-Delta Delta C(T)) calculations. Data are expressed as mean fold-change from calibrator samples as indicated in figure captions. 2(-Delta Delta C(T)) values were $\log_{10}$ transformed for statistical analysis using GraphPad Prism® software (La Jolla, CA).

Statistics. All statistics were performed using GraphPad Prism® software (La Jolla, CA). Details of statistical tests are described in figure legends.

Table S1. Immunocytochemistry primary antibodies.

Primary Antibody	Vendor	Product ID	Host Species	Isotype	Clone	Dilution	Secondary[a]
Albumin[b]	Bethyl Laboratories	A110-134A	sheep	polyclonal	n/a	1:1000	□-sheep 546
EpCAM	Origene	TA303586	rabbit	Polyclonal	n/a	1:100	□-rabbit 488
CD44	BD Pharmingen	554869	mouse	monoclonal IgG2a, □	OX-49	1:1000	□-mouse 488
E-cadherin [b]	BD Pharmingen	610182	mouse	monoclonal IgG2a, □	36	1:1000	□-mouse 488
Desmin [b]	Abcam	ab8592	rabbit	Polyclonal	n/a	1:1000	□-rabbit 488
AFP	Santa Cruz	sc-8108	goat	Polyclonal	n/a	1:50	□-goat 546

[a] refers to AlexaFluor congugated donkey □-IgG secondary antibodies utilized in quantitative imaging studies.

[b] primary antibodies utilized in high-content image analysis studies. Albumin, E-cadherin and desmin primary antibodies were used in conjuction with AlexaFluor 546, AlexaFluor 488 and AlexaFluor 647 donkey □-IgG antibodies, respectively.

Table S2. TaqMan qRT-PCR gene expression assays

Gene Symbol	NCBI GenBank mRNA	TaqMan Assay ID	Exon Boundary	Amplicon Length
Rps18 [a]	NM_213557.1	Rn01428915_g1	3-4	73
EpCAM	NM_138541.1	Rn01473202_m1	7-8	117
AFP	NM_012493.2	Rn00560661_m1	3-4	81
Alb	NM_134326.2	Rn00592480_m1	6-7	96
Ncam1	NM_031521.1	Rn00580526_m1	14-15	66
Sox17	NM_001107902.1	Rn01749232_g1	3-4	63
Sox9	AB073720.1	Rn01751069_mH	1-2	60
Ahr	NM_013149.2	Rn00682057_m1	9-10	67
Ahrr	NM_001024285.1	Rn01537444_m1	7-8	153
Cyp1a1	NM_012540.2	Rn00487218_m1	2-3	120

[a] Internal control gene.

1

Supplement Table 3. Markers in Stem/Progenitors and their Descendants (findings identical in rats and humans except where indicated)				
	Maturational Lineage Stages from Primitive Stem Cells → Adult Cells			
Epithelia	**Biliary Tree Stem Cell Subpopulations (BTSCs)***	**Intra-hepatic Stem Cells (HpSCs)**	**Hepatoblasts (HBs)**	**Hepatocytes and Cholangiocystes**
Mesenchymal Cell Partners	**Not yet defined**	**Angioblasts**	**Precursors to endothelia and to stellate cells**	**Sinusoidal endothelia-hepatocytes; stages of stellate cells-cholangiocytes**
Marker(s)	**Expression of the marker(s) in the epithelial lineage stages**			
SOX 9	Positive			Not expressed
SOX 17	Strongly expressed	Moderate levels in humans; variably expressed in rats	Negative	Negative
PDX1	Positive	Negative		
Pluripotency genes**	Strongly expressed	Moderate levels	Negative	Negative
Cytokeratins 8, 18	Positive at all stages			
Cytokeratin 19	Positive			Found on mature biliary epithelia but not on mature hepatocytes
Cytokeratin 7	Negative		Positive	Found in biliary epithelia but not hepatocytes
E-cadherin	Positive but with various patterns of expression that are lineage-stage specific			
CD133	Positive at all stem/progenitor cell stages; levels of expression decline with maturation			Negative
Hedgehog proteins (Indian, Sonic) and their receptor, patched				Negative
Telomerase	Not yet assayed in BTSCs	Protein entirely in nucleus; basal	Found partially in nucleus and	protein found entirely in cytoplasm. No activity

		level of telomerase activity	cytoplasm; telomerase activity 5X higher	except in regenerative responses; assumption that some telomerase is translocated to the nucleus during regeneration
LGR5	Most BTSC subpopulations are negative; those that are positive are at intermediate stages	Positive	Positive/weak	Negative
EpCAM		Found throughout the cell	Found only at the plasma membrane	Found on mature biliary epithelia
NCAM	positive		Negative	Negative
ICAM-1	Negative	Negative	Positive on epithelia and on sinusoidal endothelia)	Positive (levels increase with maturation)
Albumin	Negative	Minimal levels (if any); variable numbers of cells positive	All cells are positive (albeit at low levels)	much higher levels in hepatocytes but not expressed in biliary epithelia
Alpha-fetoprotein	Negative	Negative	Strongly expressed	Negative
Transferrin	Not yet assayed	Positive for transferrin mRNA but not for the protein		Positive for both mRNA and protein
Connexins	Not yet assayed	None	Connexins 28 and 43	Connexin 32
P450s	Not yet assayed	None	P450A7	P450s 3A and many others (zonal distribution)
Endothelial cell Markers (e.g. CD31, Von Willebrand Factor)	Negative			
Hemopoietic cell markers (e.g. CD34, CD45, red blood cell antigen)	Negative			
Mesenchymal Cell Markers	Negative			

(e.g. *desmin*, alpha-smooth muscle actin, CD146, CD90)	
There are at least 3 major lineage stages of biliary tree stem cell subpopulations, and more are being identified with ongoing studies; these transition to either hepatic stem cells or pancreatic stem cells. See schematic of the subpopulations on page 6	
**Pluripotency genes: OCT4, SOX2, NANOG, KLF4, SALL4	
The findings summarized above are either from the studies reported in this manuscript or are those from prior reports on rodent livers (20, 34, 40, 41) or on human livers (7, 18, 19, 22, 37, 38, 42, 43) or human biliary tree (9, 14, 15, 17) . See also in recent reviews (6, 9-11)	

Fig. S1. Chemical structures of AHR agonists. (A) 2,3,7,8-tetrachlorodibenzo-p-dioxin (TCDD), B) 6-formylindolo[2,3-b]carbazole (FICZ), C) 3,3'-diindolylmethane (DIM).

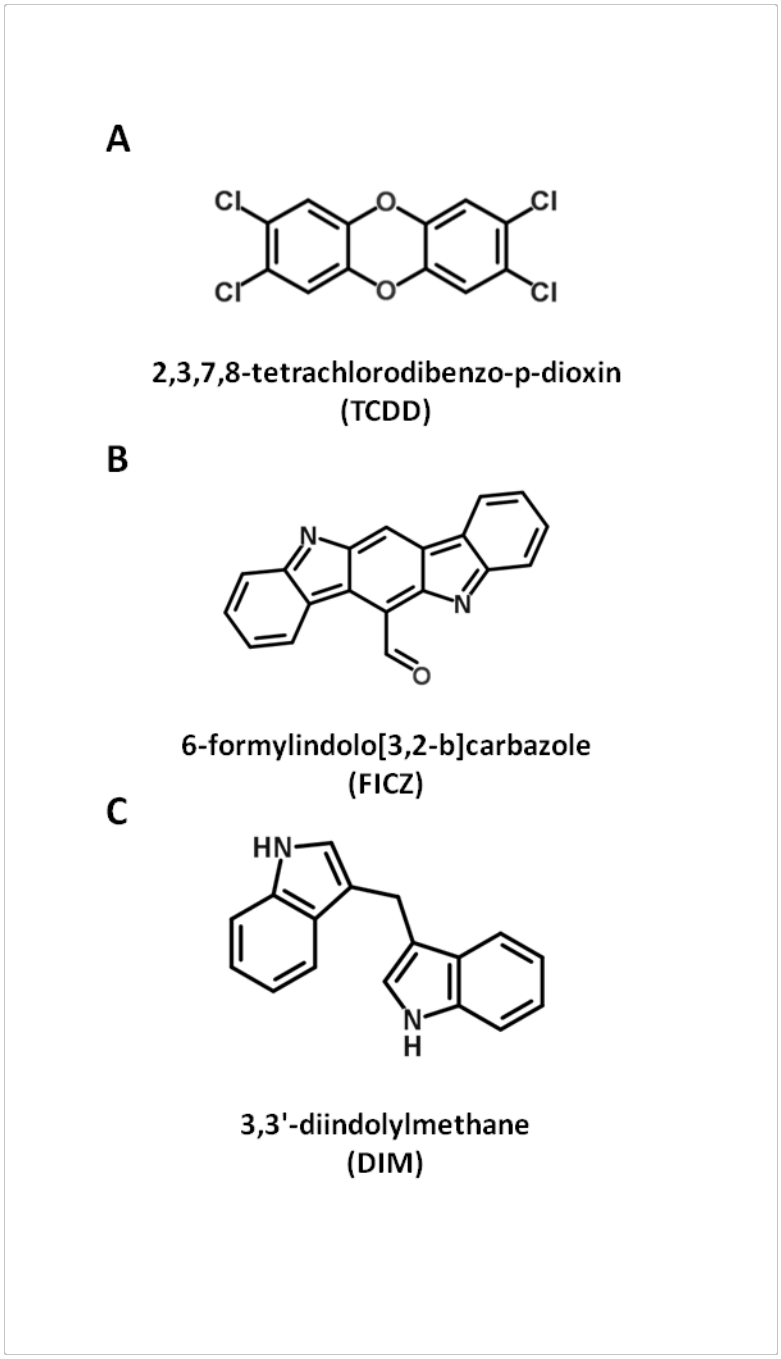

Fig. S2. Schematic of AHR Signaling.(44-54)

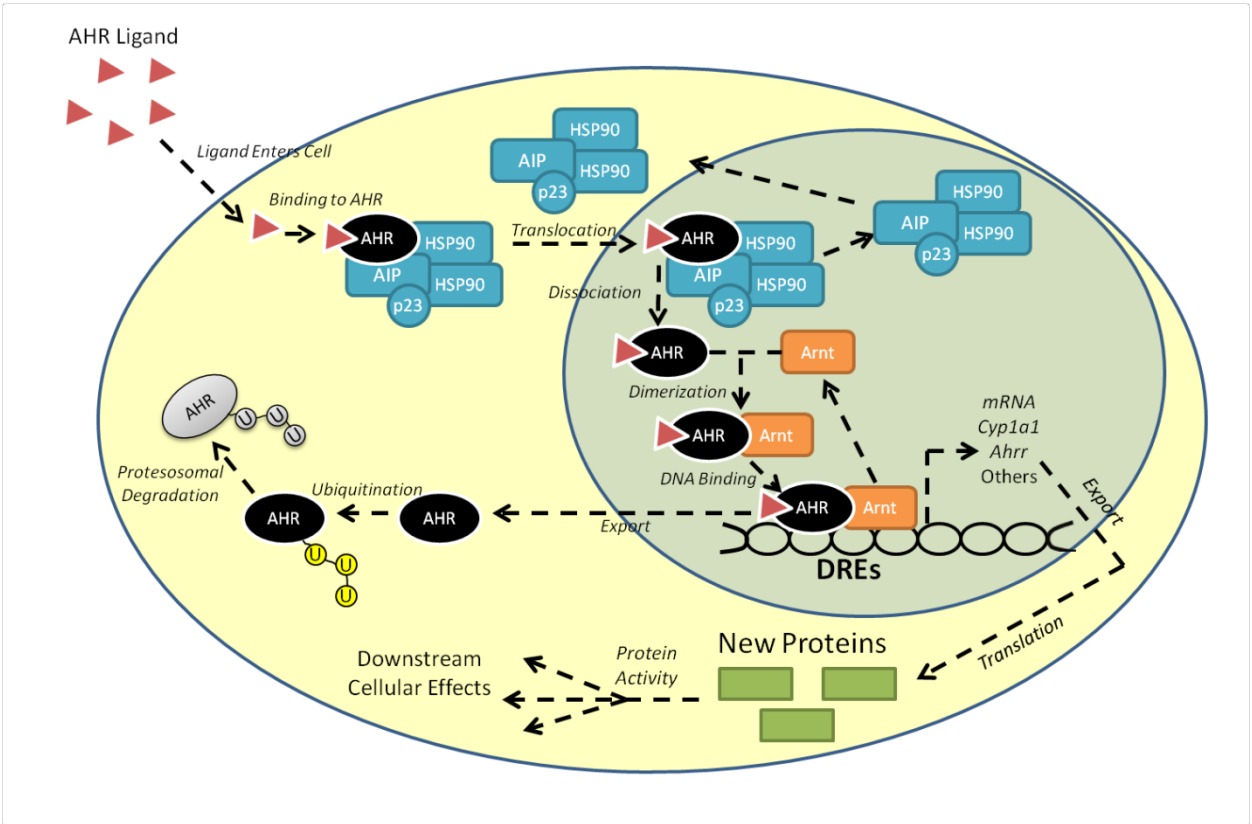

Fig. S3. Quantitative analysis of rat hepatic stem/progenitor cell growth in the presence of leukemia inhibitory factor. Rat hepatic stem / progenitors were cultured on 30 μg/cm^2 hyaluronan in KM plus varying concentrations of LIF for 3, 6, 9 or 12 days *in vitro*. At each time point, cultures were sampled and immunolabeled with E-cadherin (green), albumin (red) and Hoechst 33528 to visualize nuclei (blue). (A) Pseudo-colored composite image. (B) E-cadherin image. (C) E-cadherin object identification: E-cadherin labeling was used to identify hepatic stem/progenitor colonies as bright objects on a dark background. Fluorescent intensity and geometric gating parameters were set to reliably trace the border of E-cadherin+ colonies (blue outlines = selected objects). Fluorescent intensity measurements for E-cadherin were also calculated within each selected object mask and used at later stages of analysis. (D) Albumin image. (E) Albumin intensity quantification: positional coordinates from the E-cadherin trace were super-imposed upon the albumin image in order to obtain fluorescent intensity measurements used at later stages of analysis. (F) Nucleus image. (G) Nucleus identification: positional coordinates from the E-cadherin trace were super-imposed upon the nucleus image. Nuclei contained within the mask for each selected colony were identified as bright objects on a dark background (green mask) and counted.

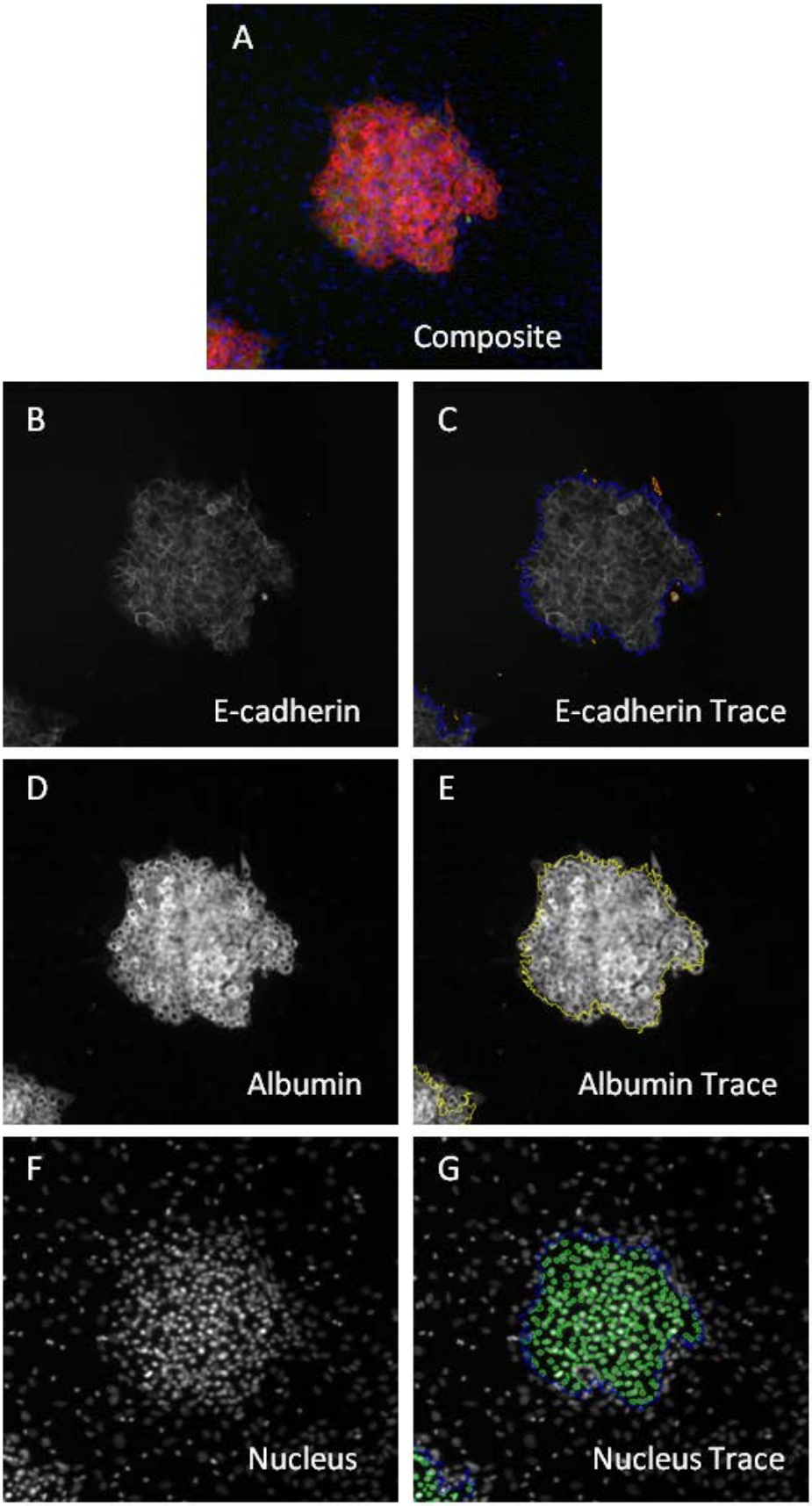
A
Composite
B
E-cadherin
C
E-cadherin Trace
D
Albumin
E
Albumin Trace
F
Nucleus
G
Nucleus Trace

1

Fig. S4. Quantitative analysis of rat stellate precursor cell growth in the presence of leukemia inhibitory factor. Rat hepatic stem / progenitors were cultured on 30 µg/cm^2 hyaluronan in KM plus varying concentrations of LIF for 3, 6, 9 or 12 days *in vitro*. At each time point, cultures were sampled and immunolabeled with desmin (yellow) + Hoechst 33258 to visualize nuclei (cyan). (A) Pseudo-colored composite image. (B) Desmin image. (C) Desmin object identification: desmin+cells were identified as bright objects on a dark background. Fluorescent intensity and geometric gating parameters were set to reliably trace desmin-positive cells (blue outlines = selected objects). Small areas of green immunofluorence which did not correspond to a definitive nucleus were excluded from analysis (orange outlines = rejected objects). (D) Nucleus image. (E) Nucleus identification: positional coordinates from the desmin trace were super-imposed upon the nucleus image. Nuclei contained within a selected desmin+ cell were quantified (red mask).

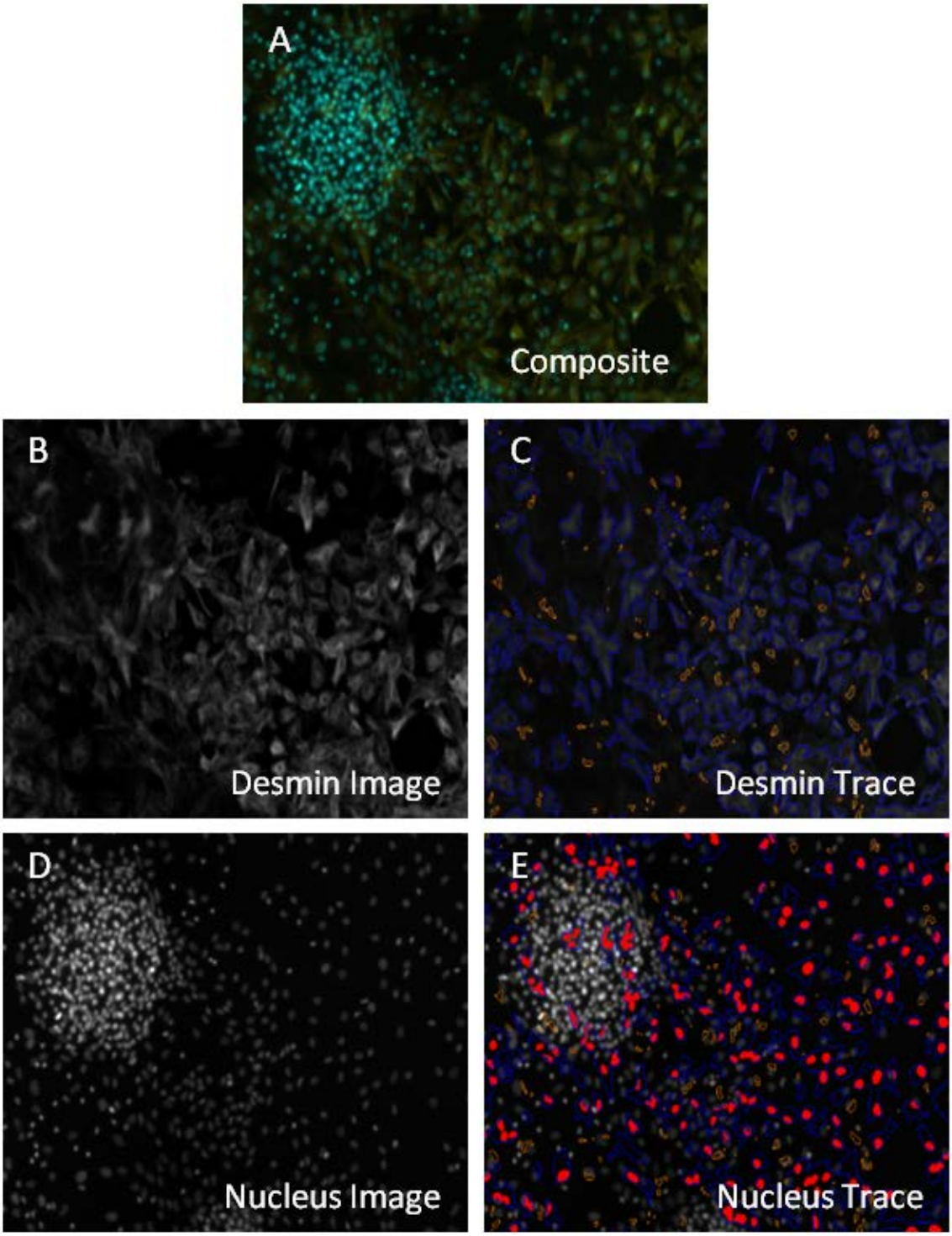
A
Composite
B
Desmin Image
C
Desmin Trace
D
Nucleus Image
E
Nucleus Trace

Fig. S5. Growth rat hepatic stem/progenitor cultures on tissue culture plastic, collagen III or collagen IV. Rat hepatic stem / progenitors were cultured on either tissue culture plastic (top row), 5 µg/cm^2 collagen III (middle row) or 5 µg/cm^2 collagen IV (bottom row) for 3 (left column), 7 (middle column) or 10 (right column) days *in vitro*. Cells were plated in serum-free Kubota's media and allowed a 48 h attachment period at which time, unattached cells were rinsed away. Growth of the culture was monitored using phase-contrast microscopy. The panels are representative images of epithelial cell clusters (arrows) and surrounding mesenchymal (arrowhead) or endothelial (asterisk) cells. In each case, mesenchymal and/or endothelial cell overgrowth of cultures occurred and epithelial cell growth was limited. Scale bar = 100 µm.

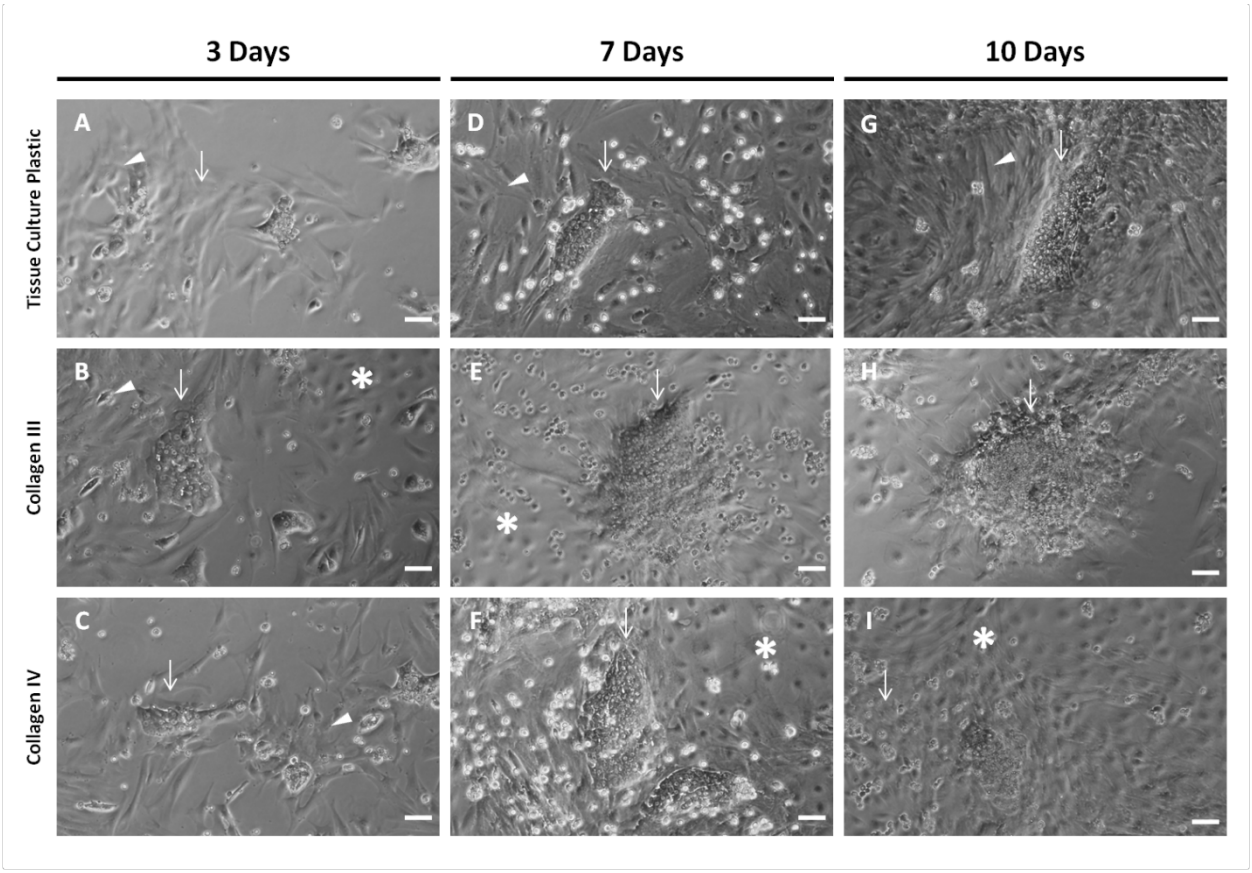

Fig S6. Expression patterns of hepatic stem/progenitor cell markers in adult rat hepatocytes. Images are matching phase contrast and pseudocolored fluorescent images. (A-A') CD44H. (B-B') E-Cadherin. (C-C') EpCAM. (D-D') AFP. (E-E') Albumin. (F-F') Desmin. Scale bar = 50 µm.

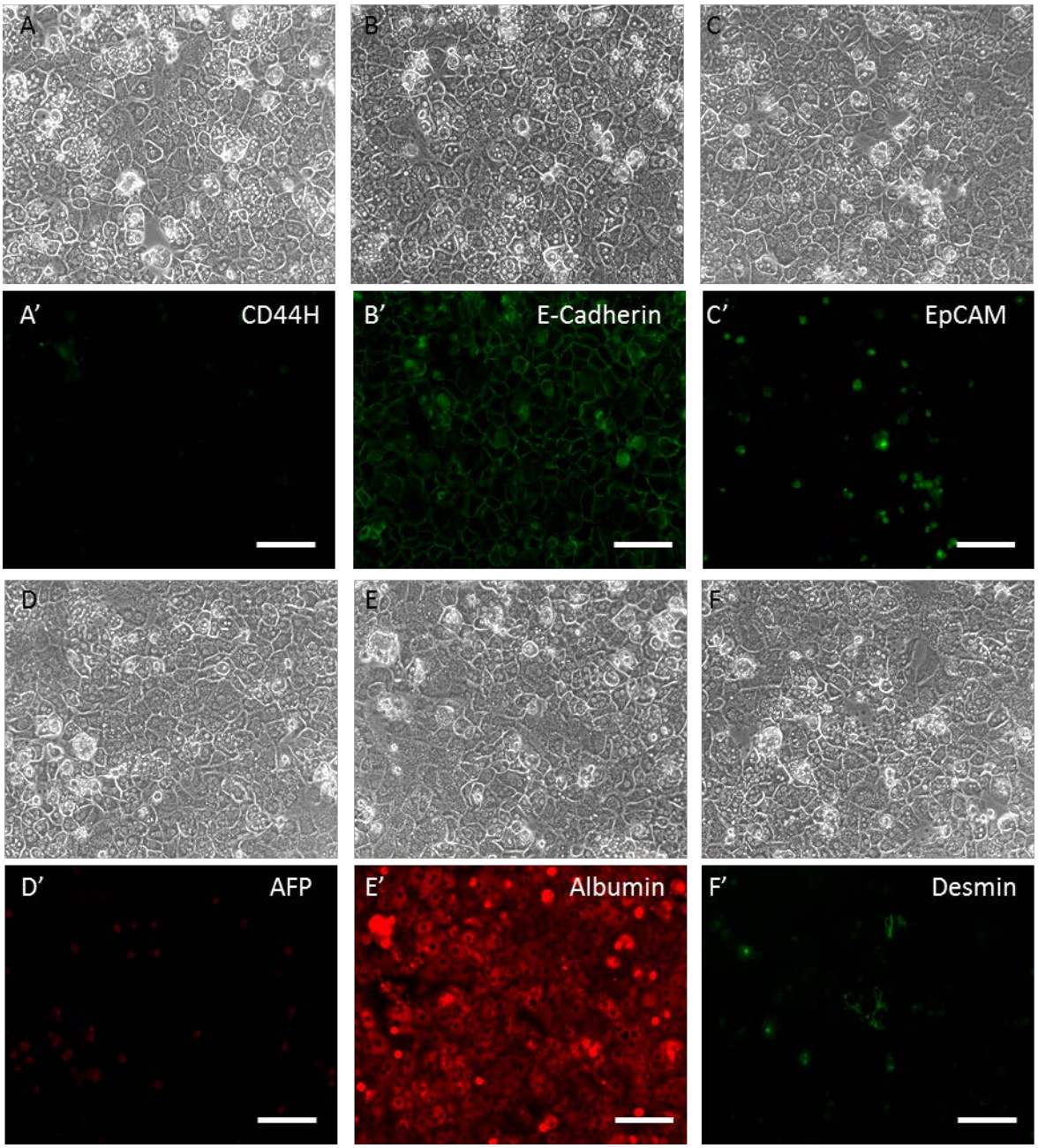

1

2

References

1. Gumucio JJ, editor. Hepatocyte heterogeneity and liver function. Madrid: Springer International; 1989.
2. Traber PG, Chianale J, Gumucio JJ. Physiologic significance and regulation of hepatocellular heterogeneity [see comments]. Gastroenterology 1988;95:1130-1143.
3. Jungermann K, Katz N. Functional specialization of different hepatocyte populations. [Review] [387 refs]. PHYSIOLOGICAL REVIEWS 1989;69:708-764.
4. Gebhardt R. Heterogeneous intrahepatic distribution of glutamine synthetase. Acta Histochem Suppl 1990;40:23-28.
5. Gebhardt R, Lindros K, Lamers WH, Moorman AF. Hepatocellular heterogeneity in ammonia metabolism: demonstration of limited colocalization of carbamoylphosphate synthetase and glutamine synthetase. Eur J Cell Biol 1991;56:464-467.
6. Turner R, Lozoya O, Wang YF, Cardinale V, Gaudio E, Alpini G, Mendel G, et al. Hepatic stem cells and maturational liver lineage biology. Hepatology 2011;53:1035-1045.
7. *Schmelzer E, *Zhang L, Bruce A, E. W, Ludlow J, Yao H, Moss N, et al. Human hepatic stem cells from fetal and postnatal donors. Journal of Experimental Medicine 2007;204:1973-1987. (*co-equal first authors)
8. Wauthier E, McClelland R, Turner W, Schmelzer E, Kubota H, Zhang L, Ludlow J, et al. Hepatic stem cells and hepatoblasts: identification, isolation and *ex vivo* maintenance Methods for Cell Biology (Methods for Stem Cells) 2008;86:137-225.
9. Cardinale V, Wang Y, Gaudio E, Carpino G, Mendel G, Alpini G, Reid LM, et al. The Biliary Tree: a Reservoir of Multipotent Stem Cells. Nature Reviews-Gastroenterology and Hepatology 2012;9:231-240.
10. Furth ME, Wang Y, Cardinale V, Carpino G, Lanzoni G, Cui C-B, Wauthier E, et al.: Stem Cell Populations Giving Rise to Liver, Biliary Tree and Pancreas. In: Sell S, ed. The Stem

Cells Handbook, 2nd Edition. Volume In Press. New York City, New York: Springer Science Publishers, NY, NY, 2013.

11. Lanzoni G, Cui C, Oikawa T, Wang Y, Carpino G, Cardinale V, Gabriel M, et al. Clinical Programs of Stem Cell Therapies for Liver and Pancreas. Stem Cells 2013;In Press.

12. Alpini G, Roberts S, Kuntz SM, Ueno Y, Gubba S, Podila PV, LeSage G, et al. Morphological, molecular, and functional heterogeneity of cholangiocytes from normal rat liver. Gastroenterology 1996;10:1636-1643.

13. Alpini G, Glaser S, Robertson W, Rodgers RE, Phinizy JL, Lasater J, LeSage GD. Large but not small intrahepatic bile ducts are involved in secretin-regulated ductal bile secretion. The American Journal of Physiology. 1997;272:G1064-G1074.

14. Carpino G, Cardinale V, Gentile R, Onori P, Semeraro R, Franchitto A, Wang Y, et al. Human gallbladder contains multipotent stem/progenitor cells. Journal of Hepatology 2014;60:1194-2020.

15. *Carpino G, *Cardinale V, Onori P, Franchitto A, Bartolomeo Berloco P, Rossi M, Wang Y, et al. Biliary tree stem/progenitor cells in glands of extrahepatic and intraheptic bile ducts: an anatomical *in situ* study yielding evidence of maturational lineages. Journal of Anatomy 2012;220:186-199. (*co-equal first authors)

16. Wang Y, *Lanzoni G, *Carpino G, Cui C, Dominguez-Bendala J, Wauthier E, Cardinale V, et al. Biliary Tree Stem Cells, Precursors to Pancreatic Committed Progenitors: Evidence for Life-long Pancreatic Organogenesis. . Stem Cells 2013;31:1966-1979. . (*co-equal authors0

17. *Cardinale V, *Wang Y, Carpino G, Cui C, Inverardi L, Dominguez-Bendala J, Ricordi C, et al. Multipotent stem cells in the extrahepatic biliary tree give rise to hepatocytes, bile ducts and pancreatic islets. Hepatology 2011;54:2159-2172. (*co-equal first authors)

18. Zhang L, Theise N, Chua M, Reid LM. Human hepatic stem cells and hepatoblasts: Symmetry between Liver Development and Liver Regeneration. Hepatology 2008;48:1598-1607.

19. Schmelzer E, Wauthier E, Reid LM. Phenotypes of pluripotent human hepatic progenitors. Stem Cell 2006;24:1852-1858.

20. Kubota H, Yao H, Reid LM. Identification and characterization of vitamin A-storing cells in fetal liver. Stem Cell 2007;25:2339-2349.

21. Wang Y, Yao H, Barbier C, Wauthier E, Cui C, Moss N, Yamauchi M, et al. Lineage-Dependent Epithelial-Mesenchymal Paracrine Signals Dictate Growth versus Differentiation of Human Hepatic Stem Cells to Adult Fates. Hepatology 2010;52:1443-1454.

22. Schmelzer E, Reid LM. Telomerase activity in human hepatic stem cells , hepatoblasts and hepatocytes from neonatal, pediatric, adult and geriatric donors. European Journal of Hepatology and Gastroenterology 2009;21:1191-1198.

23. Theise ND, Saxena R, Portmann BC, Thung SN, Yee H, Chiriboga L, Kumar A, et al. The canals of Hering and hepatic stem cells in humans. Hepatology 1999;30:1425-1433.

24. Kuwahara R, Kofman AV, Landis CS, Swenson ES, Barendswaard E, Theise ND. The hepatic stem cell niche: identification by label retaining cell assay. Hepatology 2008;47:1994-2002.

25. Lindros KO, Oinonen T, Issakainen J, Nagy P, Thorgeirsson SS. Zonal distribution of transcripts of four hepatic transcription factors in the mature rat liver. Cell Biol Toxicol 1997;13:257-262.

26. Lindros KO. Zonation of cytochrome P450 expression, drug metabolism and toxicity in liver. General Pharmacology: The Vascular System 1997;28:191-196.

27. Gebhardt R, Alber J, Wegner H, Mecke D. Different drug metabolizing capacities in cultured periportal and pericentral hepatocytes. Biochem Pharmacol 1994;48:761-766.

28. Jungermann K, Kietzmann T. Zonation of parenchymal and nonparenchymal metabolism in liver. Annual Review on Nutrition 1996;16:179-203.

29. Jungermann K. Functional heterogeneity of periportal and perivenous hepatocytes. [Review] [135 refs]. Enzyme 1986;35:161-180.

30. Sigal SH, Gupta S, Gebhard DF, Jr., Holst P, Neufeld D, Reid LM. Evidence for a terminal differentiation process in the rat liver. Differentiation 1995;59:35-42.

31. Sigal SH, Rajvanshi P, Gorla GR, Sokhi RP, Saxena R, Gebhard DR, Jr., Reid LM, et al. Partial hepatectomy-induced polyploidy attenuates hepatocyte replication and activates cell aging events. American Journal of Physiology - Gastrointestinal and Liver Physiology 1999;276:G1260-1272.

32. Twisk J, Hoekman MF, Mager WH, Moorman AF, de Boer PA, Scheja L, Princen HM, et al. Heterogeneous expression of cholesterol 7 alpha-hydroxylase and sterol 27-hydroxylase genes in the rat liver lobulus. J Clin Invest 1995;95:1235-1243.

33. Kuo FC, Darnell JE, Jr. Evidence that interaction of hepatocytes with the collecting (hepatic) veins triggers position-specific transcription of the glutamine synthetase and ornithine aminotransferase genes in the mouse liver. Mol Cell Biol 1991;11:6050-6058.

34. Kubota H, Reid LM. Clonogenic hepatoblasts, common precursors for hepatocytic and biliary lineages, are lacking classical major histocompatibility complex class I antigens. Proc. Natl. Acad. Sci. (USA) 2000;97:12132-12137.

35. McClelland R, Wauthier E, Zhang L, Barbier C, Melhem A, Schmelzer E, Reid LM. *Ex vivo* conditions for self-replication of human hepatic stem cells Tissue Engineering 2008;14:1-11.

36. Semeraro R, Carpino G, Cardinale V, Onori P, Gentile R, Cantafora A, Franchitto A, et al. Multipotent Stem/Progenitor Cells in the Human Foetal Biliary Tree. Journal of Hepatology 2012;220 186-199.

37. Turner WS, Schmelzer E, McClelland R, Wauthier E, Chen W, Reid LM. Human hepatoblast phenotype maintained by hyaluronan hydrogels. Journal of Biomedical Materials 2007;82:156-168.

38. Turner WS, Seagle C, Galanko J, Favorov O, Prestwich GD, Macdonald JM, Reid LM. Metabolomic Footprinting of Human Hepatic Stem cells and Hepatoblasts Cultured in Engineered Hyaluronan-Matrix Hydrogel Scaffolds. Stem Cell 2008;26:1547-1555.

39. Livak KJ, Schmittgen TD. Analysis of relative gene expression data using real-time quantitative PCR and the 2 (-Delata Deelta C (T)) Method. Methods 2001;25:402-.

40. Sigal SH, Brill S, Reid LM, Zvibel I, Gupta S, Hixson D, Faris R, et al. Characterization and enrichment of fetal rat hepatoblasts by immunoadsorption ("panning") and fluorescence-activated cell sorting. Hepatology 1994;19:999-1006.

41. Kubota H, Storms RW, Reid LM. Variant forms of alpha-fetoprotein transcripts expressed in human hematopoietic progenitors. Implications for their developmental potential towards endoderm. Journal of Biological Chemistry 2002;277:27629-27635.

42. Schmelzer E, Reid LM. EpCAM Expression in Normal, Non-Pathological Tissues. Frontiers in Biosciences 2008;13:3096-3100.

43. Oikawa T, *Kamiya A, Zeniya M, Chikada H, Hyuck AD, Yamazaki Y, Wauthier E, et al. SALL4, a stem cell biomarker in liver cancers. Hepatology 2013;57:1469-1483.

44. Gu YZ, Hogenesch JB, Bradfield CA. The PAS superfamily: sensors of environmental and developmental signals. Annual Review in Pharmacology and Toxicology 2000;40:519-561.

45. Beischlag TV, Luis Morales J, Hollingshead BD, Perdew GH. The aryl hydrocarbon receptor complex and the control of gene expression. Critical Reviews of Eukaryotic Gene Expression 2008;18:207-250.

46. Hankinson O. The aryl hydrocarbon receptor complex. Annual Reviews in Pharmacology and Toxicology 1995;35:307-340.

47. Ikuta T, Tachibana T, Watanabe J, al. e. Nucleocytoplasmic shuttling of the aryl hydrocarbon receptor. Journal of Biochemistry 2000;127:503-509.

48. Denison MS, Fisher JM, Whitlock JP, Jr. Protein-DNA interactions at recognition sites for the dioxin-Ah receptor complex. Jouirnal of Biological Chemistry 1989;264:16478-16482.

49. Denison MS, Soshilov AA, He G, DeGroot DE, Zhao B. Exactly the same but different: promiscuity and diversity in the molecular mechanisms of action of the aryl hydrocarbon (dioxin) receptor. Toxicology Science 2011;124:1-22.

50. Durrin LK, Jones PB, Fisher JM, Galeazzi DR, Whitlock JPJ. 2,3,7,8-Tetrachlorodibenzo-p-dioxin receptors regulate transcription of the ctuchrome P1-450 gene. Journal of Cell Biochemistry 1987;35:153-160.

51. Quattrochi LC, Vu T, Tukey RH. The human CYP1A2 gene and induction by 3-methylcholanthrene. A region of DNA that supports AH-receptor binding and promoter-specific induction. Journal of Biological Chemistry 1994;269:6949-6954.

52. Baba T, Mimura J, Gradin K, Kuroiwa A, Watanabe T, Matsuda Y, Inazawa J, et al. Structure and expression of the Ah receptor repressor gene. Journal of Biological Chemistry 2001;276:33101-33110.

53. Prochazkova J, Kabatkova M, Bryja V, Umannová L, Bernatík O, Kozubík A, Machala M, et al. The interplay of the aryl hydrocarbon receptor and bveta-catenin alters both AhR-dependent transcription and Wnt/beta-catenin signaling in liver progenitors. Toxicol Sciences 2011;122:249-360.

54. Prochazkova J, Kozubik A, Machala M, Vondráček J. Differential effects of indirubin and 2,3,7,8-tetrachlorodibenzo-p-dioxin on the aryl hydrocarbon receptor (AhR) signaling in liver progenitor cells. Toxicology 2011;279:146-154.